Charge-Transfer Spectrum and Its Temperature Dependence in La_2CuO_4

J. P. Falck, A. Levy, M. A. Kastner, and R. J. Birgeneau
Department of Physics, Massachusetts Institute of Technology, Cambridge, Massachusetts 02139
(Received 4 May 1992)

The reflectivity and its temperature dependence in the neighborhood of the charge-transfer band is reported for carrier-free La_2CuO_4. There is a sharp peak in the imaginary part of the dielectric function for light polarized parallel to the CuO_2 layers. It is shown that the line shape as well as its temperature dependence is consistent with short-range electron-hole interaction in the final state of the charge-transfer excitation broadened by moderate coupling to optical phonons.

PACS numbers: 74.65.+n, 63.20.Kr, 78.20.Ci

La_2CuO_4 is one of the simplest antiferromagnetic semiconductors into which introduction of charge carriers gives rise to high-temperature superconductivity. Accordingly, the elementary electronic excitations of La_2CuO_4 have received a great deal of attention [1,2]. A variety of spectroscopies [3] show that the lowest-energy electronic excitations correspond to the transfer of electrons from O to Cu in the CuO_2 layer. Thus, the material is a charge-transfer insulator. These excitations are especially interesting because they play a central role in multiband Hubbard models used to describe the insulating as well as the superconducting material. However, the spectrum of the charge-transfer excitations is peculiar. On the one hand, the spectrum consists of a rather sharp peak near the band edge which disappears with doping. In the literature this feature is often interpreted as a bound exciton [2,4]. On the other hand, the observation of photoconductivity in the same spectral region [5] demonstrates that the excitations result in separated electrons and holes.

Surprisingly, the spectrum of these charge-transfer excitations has not been studied as a function of temperature. Further, there is no satisfactory model for the excitation line shape. We report here measurements of that spectrum and its temperature dependence. A theory in which the final state consists of electron and hole polarons coupled to each other by a short-range potential provides an excellent fit to the data at low temperatures and predicts the spectrum up to ~ 400 K with no adjustable parameters. Because the theory requires that charge carriers are coupled to longitudinal optical phonons, our results have important implications for doped La_2CuO_4.

Single crystals of pure La_2CuO_4 were grown by the top-seeded solution growth method using CuO flux [6]. As grown, the crystals contained a density of $\sim 4\times 10^{19}$ cm^{-3} holes due to doping by oxygen acceptors, sufficient to reduce the Néel temperature to $T_N \simeq 240$ K. The crystals were reduced by annealing at 1170 K for 30 min in a vacuum increasing the Néel temperature to 325 K. A sharp peak at T_N in the magnetic susceptibility indicated a homogeneous oxygen concentration. The crystals with area ~ 5 mm^2 and thickness ~ 2 mm were cut and oriented with a tetragonal (100) surface. The annealing process is known to deplete the surface of copper to a depth of roughly 2 μm. Therefore, several micrometers were ground off before polishing, and the surfaces were subsequently etched for 20 min in a solution of 1% Br in methanol. The 2-eV in-plane reflectivity peak was found to become sharper the longer the crystal was etched, saturating at roughly 20 min.

The reflectivity spectrum was measured at $\sim 10°$ incidence on the (100) tetragonal surface in the energy range 0.5–3.1 eV. The reflectivity was normalized to that of an Al mirror, whose absolute reflectivity was measured by removing it and placing the detector in the incident beam. The accuracy of the absolute reflectivity is ~ 0.05. The complex dielectric function was calculated from the reflectivity using the Kramers-Krönig transformations. For the low-energy extrapolation ($\hbar\omega < 0.5$ eV) we assumed a constant reflectivity. At high energies ($\hbar\omega > 3.0$ eV) we matched published ultraviolet single-crystal reflectivity data [2] to our spectra.

Figure 1(a) shows spectra of the optical reflectivity at 122 and 447 K for polarization parallel and perpendicular to the CuO_2 sheets. The prominent charge-transfer feature near 2.0 eV is observed only for the in-plane spectrum. The out-of-plane spectrum shows no structure in this energy region demonstrating the 2D nature of the excitations. The charge-transfer peak is seen to sharpen and move to higher energies upon cooling. At $T \sim 120$ K this evolution saturates and further cooling alters neither the position nor the width of the peak. The shift of the in-plane reflectivity peak is shown in Fig. 2. Cooling from 450 K, the peak position increases linearly with decreasing temperature at a rate of 6.8×10^{-4} eV/K before it saturates at $T \sim 120$ K. This evolution is similar to that reported for $YBa_2Cu_3O_6$ powder samples [4].

In addition to the charge-transfer peak, a kink in the reflectivity near 1.75 eV is observed in the in-plane spectrum. This feature, observed in several samples, is only resolved at low temperatures and only in high-resistivity crystals which probably explains why it has not been seen in previous measurements [1,2].

The imaginary part of the dielectric function, ϵ_2, at 122 K for the in-plane spectrum is shown in Fig. 1(b), together with the photoconductivity at 132 K for an identically

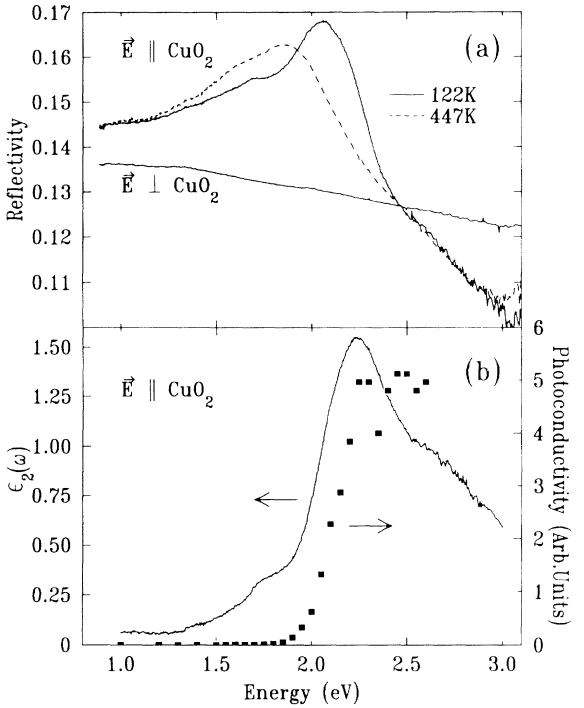

FIG. 1. (a) Reflectivity spectra of La_2CuO_4 at $T=122$ and 447 K. (b) In-plane $\epsilon_2(\omega)$ at $T=122$ K together with the photoconductivity at $T=132$ K on an identically prepared sample (from Ref. [5]).

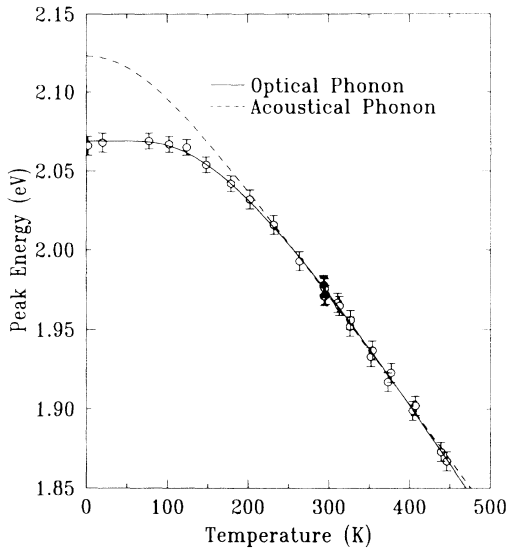

FIG. 2. The temperature dependence of the reflectivity peak. The solid and dashed lines represent the best fits to an edge shift induced by optical and acoustic phonons, respectively.

prepared crystal [5]. The peak in ϵ_2, at 2.25 eV, has a total width of only ~ 0.4 eV. The photoconductivity has a threshold coinciding with that of the ϵ_2 peak, indicating that the absorption is associated with the creation of free electrons and holes. The plateau on the low-energy side of the 2.0-eV absorption edge results from the kink in the reflectivity [Fig. 1(a)]. This second excitation, centered at 1.75 eV, has no associated photoconductivity indicating that the absorption results in the creation of excitons.

Even though the absorption above 2 eV leads to separated electron-hole pairs, the narrowness of the peak at 2.25 eV indicates that the interaction between the electron and hole is important in the interband transitions as well as in those of the bound exciton. It is well known that the electron-hole interaction enhances matrix elements for interband transitions at low energies. In 2D [7] this enhancement is more dramatic than in 3D [8]. However, even in 2D the Coulomb interaction cannot account for the sharp peak we observe. It leads, instead, to an enhanced absorption over a range of energies corresponding to ~ 10 times the excition binding energy.

By assuming a short-range interaction between electrons and holes we find a consistent description of the peak in ϵ_2. Such an interaction is appropriate for Frenkel excitons, like those in solid rare gases and molecular crystals, rather than for the Mott-Wannier variety which are spread out over many unit cells, as in conventional semiconductors. For the simplest model $V(\mathbf{r})=-g\delta(\mathbf{r})$, where $\mathbf{r}$ is the separation of the electron and hole, the problem can be solved exactly [7]. The resulting dielectric constant is

$$\epsilon_2(\omega) \propto |1-gF(\omega)|^{-2}\mathrm{Im}F(\omega)\,, \tag{1}$$

where

$$F(\omega)=-\lim_{\eta\to 0}\int_0^\infty \frac{D(\omega')d\omega'}{\omega-\omega'+i\eta}\,. \tag{2}$$

Here $D(\omega)$ is the joint density of states, which in 2D is $\mu/\pi\hbar^2$ above the band gap, where μ is the reduced effective mass of electron and hole. In the limit of $g=0$ the dielectric function in Eq. (1) reduces to the usual result for interband transitions. The effect of the short-range electron-hole interaction is to enhance the matrix elements near threshold. Equation (1) yields sharp resonances when $|1-gF(\omega)|^2 \ll 1$.

Measurements of Chen *et al.* [9] show that the static dielectric constant in La_2CuO_4 is large enough that electrons and holes form Fröhlich polarons. For such polarons, the T dependence of the polaron self-energy causes a shift of the band edge [10] given by

$$E_g(T)=E_g^0-2\hbar\omega_0\alpha_p[n(\hbar\omega_0/k_BT)+1]\,, \tag{3}$$

where n is the Bose-Einstein occupation number. The assumption of coupling to a single LO phonon of frequency ω_0, implicit in Eq. (3), will be discussed below. The polaron coupling constant is defined as

$$\alpha_p=\frac{1}{2}\frac{e^2}{2\hbar\omega_0}\left(\frac{1}{\epsilon_\infty}-\frac{1}{\epsilon_s}\right)\left(\frac{2m\omega_0}{\hbar}\right)^{1/2}, \tag{4}$$

where ϵ_s is the static dielectric constant and ϵ_∞ the electronic contribution. For simplicity, we assume that the

electron and the hole have the same mass and hence the same α_p.

The phonon scattering also induces a decay rate of the quasiparticles. We assume that the decay rate for the correlated state of electron and hole is the sum of the individual polaron relaxation rates [11]. This gives

$$\gamma(T)=2^{3/2}\omega_0(\hbar\omega_0/E)^{1/2}\alpha_p[2n(\hbar\omega_0/k_BT)+1]. \quad (5)$$

Here E denotes the total kinetic energy of the electron and hole, that is, $\hbar\omega-E_g(T)$. This expression is valid only for $E>\hbar\omega_0$; however, the undressed ϵ_2 is small enough near $E_g(T)$ that this restriction is unimportant. We emulate the effect of the electron-phonon interaction phenomenologically by introducing the lifetime broadening into the dielectric function, replacing η in Eq. (2) with $\gamma(T)/2$ and shifting the band edge according to Eq. (3).

The presence of moderate coupling to LO phonons is illustrated by the shift of the reflectivity peak with temperature. The best fit of Eq. (3) to the data, shown as the solid curve in Fig. 2, yields $\hbar\omega_0=43\pm4$ meV. The absence of temperature dependence below 100 K results from the freeze-out of the LO phonons. For acoustic phonon coupling [12] the saturation at low temperatures would be much more gradual reflecting the continuous density of acoustic phonon modes below the Debye energy. Figure 2 displays the best fit using the known Debye temperature of $\sim$400 K [13]. Recent inelastic neutron scattering measurements [14] show optical phonon modes in La_2CuO_4 with large LO-TO splitting at the zone center, typical of phonons with large dipole moments. The energy of the respective LO phonons is in the range $\sim$35–55 meV. Thus, our measured $\hbar\omega_0=43$ meV can be interpreted as a weighted average of the frequencies of phonons that are coupled to the charge carriers. A description assuming coupling to this one effective phonon mode provides an excellent fit to all the data as shown below.

Figure 3 displays the experimental in-plane dielectric function for four temperatures together with the predictions of our model, Eqs. (1)–(5). With $\hbar\omega_0$ fixed at 43 meV, the model has four adjustable parameters: $(\mu/m_e)g$, α_p, E_g^0, and the overall scale factor. Two of these parameters, $(\mu/m_e)g$ and α_p, control the shape of $\epsilon_2(\omega)$ including its temperature dependence. To test the model, we first fitted $\epsilon_2(\omega)$ at the lowest temperature, $T=122$ K, with all four parameters adjustable. The best fit for $T=122$ K gives $(\mu/m_e)g=5.0$ eV Å^2, $\alpha_p=5.7$, and $E_g^0=2.6$ eV. As seen in Fig. 3, the model describes the measured $\epsilon_2(\omega)$ at $T=122$ K quite well. The dashed lines for $T=295$, 378, and 447 K in Fig. 3 are calculated from our model with the parameters fixed at their $T=122$ K values. With the polaron coupling constant determined by the broadening at $T=122$ K the theory predicts the change of the peak shape and its position as well as its overall strength all the way up to $T=447$ K. Clearly, the theory works very well, indeed much better

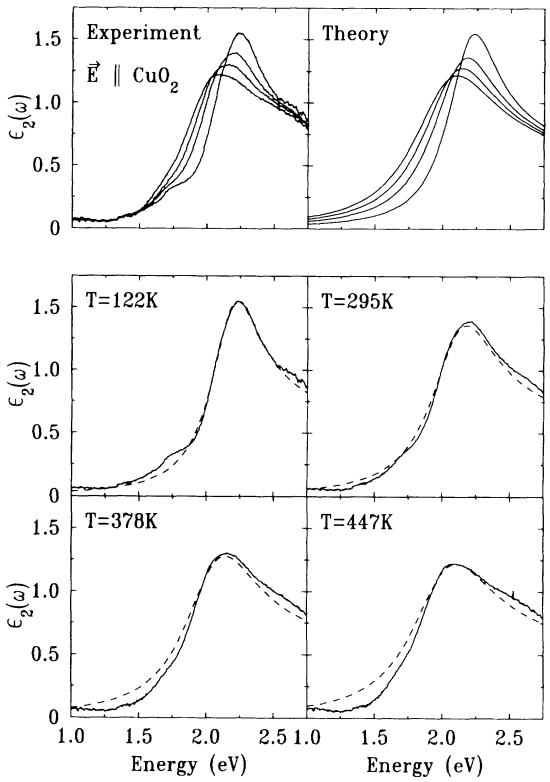

FIG. 3. The in-plane $\epsilon_2(\omega)$ for four different temperatures together with the best fit to the data using the model and the parameters discussed in the text. All four temperatures are shown in the upper panel; theory and experiment are compared for individual temperatures in the lower panel.

than one might reasonably expect given the simple form and the small number of adjustable parameters.

We find, consistent with earlier workers, that $\epsilon_\infty\simeq5$ for photon energies below $\sim$1.5 eV. With $\alpha_p=5.7$ and $\epsilon_s=30$ [9] one finds from Eq. (4) a bare mass of $\sim3.6m_e$. By including the polaron enhancement of ~2 we find a total mass of $\sim7m_e$. A proper 2D treatment of the electron-phonon coupling and inclusion of other contributions to the zero-temperature linewidth such as elastic scattering may change these numbers. 3D effects are not expected to contribute to the broadening because of the absence of any charge-transfer feature in the out-of-plane spectrum (see Fig. 1).

The parameter $E_g^0=2.6$ eV represents the bare band gap. The effective band gap differs from E_g^0 by the total electron and hole polaron self-energy. Inserting the appropriate quantities into Eq. (3) at $T=0$ K gives an energy gap for creating electron and hole polarons of $E_g(0)=2.1$ eV, in excellent agreement with the value 2.0 ± 0.1 eV from the photoconductivity [5].

To understand the origin of the short-range electron-hole interaction we describe the charge-transfer from copper to oxygen using the language of the extended Hubbard model. The effective Hamiltonian for the latter model [15] includes two kinds of interaction between a

hole on a Cu site and one on a neighboring O site. The first is the Coulomb interaction V, and the second is the exchange energy $K_{\text{eff}}\mathbf{s}\cdot\mathbf{S}$, where $\mathbf{s}$ and $\mathbf{S}$ are the spins of the holes on the oxygen and copper sites, respectively, and K_{eff} is the effective antiferromagnetic exchange. The fundamental difference between a nearest-neighbor transfer and a transfer to an oxygen site farther away is that in the latter case the hole on the oxygen site has two neighboring copper holes while for the nearest-neighbor transfer it has only one. Thus, to first order, the energy difference between a long-range and a nearest-neighbor charge transfer equals the difference in the total interaction energy between the neighboring Cu and O holes, i.e., $V+K_{\text{eff}}$. The effective interaction potential of an electron and hole can therefore be approximated by a potential well centered around the central copper ion with a depth of $\sim V+K_{\text{eff}}$ and a radius of order the Cu-O spacing. With an effective radius of ~ 2 Å and a depth of ~ 1.5 eV (see Ref. [15]) we estimate the integrated potential to be ~ 18 eV Å^2, the same order of magnitude as the value of $(\mu/m_e)g$ needed to fit the charge-transfer line shape. The observation of a bound exciton at ~ 1.75 eV is consistent with this picture. A 2D potential well of radius ~ 2 Å and depth 1.5 eV supports a bound state with a binding energy of ~ 0.2 eV. Of course, the energy of the exciton is sensitive to the details of the potential.

In summary, the charge-transfer excitation spectrum and its temperature dependence can be understood if both polaron coupling and electron-hole correlations are taken into account. Only a short-range electron-hole interaction is consistent with the charge-transfer spectrum. Furthermore, the integrated strength of this potential is of the order expected from the parameters of the extended Hubbard model. Since charges injected into La_2CuO_4 by photoexcitation form polarons, one is led to speculate, as did Chen *et al.* [9], that impurity-induced carriers are also polarons, at least at low impurity concentrations. The large dielectric constant which leads to the polaron coupling reduces the impurity potential and thus causes the insulator-to-metal transition to occur at a much lower density than it otherwise would.

We would like to thank V. Emery, D. Emin, R. E. Cohen, W. E. Pickett, and J. D. Axe for invaluable discussions. This work was supported by National Science Foundation Grants No. DMR 90-22933 and No. DMR 90-14839.

[1] J. Orenstein *et al.*, in *Novel Superconductivity*, edited by S. A. Wolf and V. Z. Dresin (Plenum, New York, 1987), p. 693; S. Tajima *et al.*, J. Opt. Soc. Am. B **6**, 475 (1989); S. L. Cooper *et al.*, Phys. Rev. B **42**, 10785 (1990).
[2] S. Uchida *et al.*, Phys. Rev. B **43**, 7942 (1991).
[3] See, for example, A. Fujimori *et al.*, Phys. Rev. B **35**, 8814 (1987).
[4] J. Humlíček, M. Garriga, and M. Cardona, Solid State Commun. **67**, 589 (1988).
[5] T. Thio *et al.*, Phys. Rev. B **42**, 10800 (1990).
[6] P. J. Picone, H. P. Jensen, and D. R. Gabbe, J. Cryst. Growth **85**, 576 (1987).
[7] B. Velický and J. Sak, Phys. Status Solidi **16**, 147 (1966).
[8] R. J. Elliott, Phys. Rev. **108**, 1384 (1957).
[9] C. Y. Chen *et al.*, Phys. Rev. B **43**, 392 (1991).
[10] H. Y. Fan, Phys. Rev. **82**, 900 (1951).
[11] H. Fröhlich, H. Pelzer, and S. Zienau, Philos. Mag. **41**, 221 (1950); J. Appel, in *Solid State Physics: Advances in Research and Applications*, edited by H. Ehrenreich, F. Seitz, and D. Turnbull (Academic, New York, 1968), Vol. 21, pp. 193–391.
[12] P. Y. Yu and M. Cardona, Phys. Rev. B **2**, 3193 (1970).
[13] S. J. Collocott *et al.*, Phys. Rev. B **36**, 5684 (1987).
[14] L. Pintschovius *et al.*, Physica (Amsterdam) **174B**, 323 (1991).
[15] V. J. Emery and G. Reiter, Phys. Rev. B **38**, 4547 (1988).